ChemComm

COMMUNICATION

View Article Online
View Journal | View Issue

Cite this: *Chem. Commun.*, 2020, **56**, 4328

Received 12th February 2020,
Accepted 5th March 2020

DOI: 10.1039/d0cc01140a

rsc.li/chemcomm

Tolerant to air σ-alkane complexes by surface modification of single crystalline solid-state molecular organometallics using vapour-phase cationic polymerisation: SMOM@polymer†

Alexander J. Bukvic,[ab] Dana Georgiana Crivoi,[b] Hollie G. Garwood,[b] Alasdair I. McKay,[b] Thomas T. D. Chen,[b] Antonio J. Martínez-Martínez[b] and Andrew S. Weller*[a]

Vapour-phase surface-initiated cationic polymerisation of ethylvinylether occurs at single-crystals of the σ-alkane complex [Rh(Cy$_2$PCH$_2$CH$_2$PCy$_2$)(NBA)][BAr$^F_4$]. This new surface interface makes these normally very air sensitive materials tolerant to air, while also allowing for onward single-crystal to single-crystal reactivity at metal sites within the lattice.

The modification of inorganic materials with covalently anchored polymer chains installs a functional interface at their surface. This allows for properties (*e.g.* chemical stability, hydrophobicity and guest exchange rates) of the resulting composite material to be systematically modified for applications in catalysis, medicine, optoelectronics, sensors, coatings and separation.[1,2] One important method for the synthesis of such hybrid materials is surface-initiated polymerisation,[3] where a surface site promotes polymer chain growth on the platform material of choice; *e.g.* 2-D surfaces,[4,5] nanoparticles,[6] metal organic frameworks (MOFs)[7,8] and supported molecular catalysts.[9] Such grafting-from methodologies are distinct from grafting-to techniques, where a preformed polymer chain is attached to a surface.[4,10] The functionalisation of discrete single-crystalline materials by surface-initiated polymerisation is, however, much less common. Such single-crystal@polymer composites have been reported for MOFs,[7] polyoxometallate frameworks (POMs),[11] benzoic acids[12] and alkali halides;[13] all of which present chemically robust platforms for surface functionalisation. Closely related work has shown that single-crystals of Co(OR)(salph) (R = Me, Ac) promote ethylene oxide polymerization, with growth occurring at specific loci on the surface of the molecular crystal rather than the whole surface.[14]

We have recently shown that addition of H_2 to the Rh-precursor [Rh(Cy$_2$PCH$_2$CH$_2$PCy$_2$)(NBD)][BAr$^F_4$], **[1-NBD][BAr$^F_4$]**, [NBD = norbornadiene, Ar^F = 3,5-(CF$_3$)$_2$C$_6$H$_3$] leads to the formation of the corresponding cationic σ-alkane[15] complex [Rh(Cy$_2$PCH$_2$CH$_2$PCy$_2$)(NBA)][BAr$^F_4$], **[1-NBA][BAr$^F_4$]** (NBA = norbornane), in a solid/gas single-crystal to single-crystal (SC–SC) reaction, Scheme 1A.[16–18] The NBA-ligand can be displaced in a further SC–SC solid/gas transformation, by substrates such as propene[17] or isobutene,[18] and this exchange is facilitated by the hydrophobic network of CF$_3$-groups in the non-porous lattice.[19] We have termed this overarching concept solid-state molecular organometallic chemistry (SMOM-chem).[17]

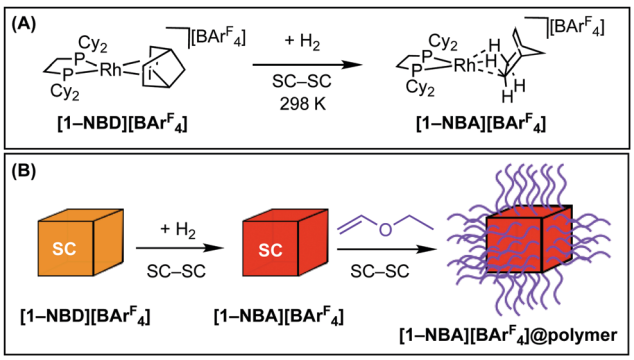

Scheme 1 (A) The SMOM-concept and generation of a σ-alkane complex. (B) Surface-initiated polymerisation to give a SMOM@polymer. SC = single crystal.

We reasoned that if this displacement initially occurred at the surface of the crystal[20] use of a volatile monomer would result in a vapour phase[13] cationic polymerisation at surface {Rh(Cy$_2$PCH$_2$CH$_2$PCy$_2$)}$^+$ initiation sites. In this contribution we report that this is the case, and that by careful control of reaction conditions single-crystallinity can be retained in this process, Scheme 1B. The polymer interface makes these normally extremely air-sensitive crystalline materials tolerant to air, and also allows for solid/gas reactivity to occur at the metal-sites within the molecular crystal, in a SC–SC transformation.

[a] *Department of Chemistry, University of York, Heslington, York, YO10 5DD, UK*
[b] *Department of Chemistry, University of Oxford, Oxford, OX1 3TA, UK.*
E-mail: andrew.weller@york.ac.uk

† Electronic supplementary information (ESI) available. CCDC 1022726, 1983128 and 1983126. For ESI and crystallographic data in CIF or other electronic format see DOI: 10.1039/d0cc01140a

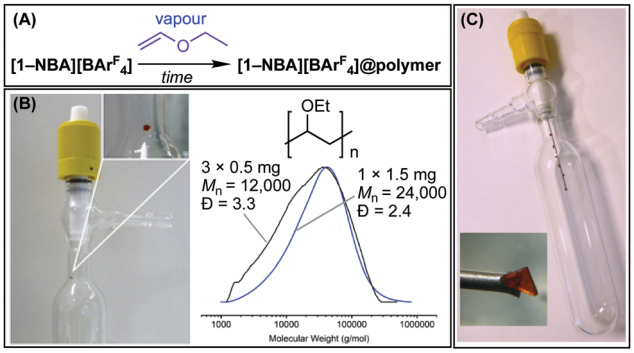

Fig. 1 (A) Vapour phase grafting-from polymerisation of EVE. (B) Experimental setup for "Method A". Overlaid GPC traces, from single experiments, of polymer formed using 1.5 mg crystals **[1-NBA][BArF4]** formed by addition of H_2 to **[1-NBD][BArF4]** of different sizes [THF, 10 mg ml^{-1}, M_n (g mol^{-1}) relative to polystyrene standards]. (C) Experimental setup for "Method B", inset shows single-crystal mounting of **[1-NBA][BArF4]@polymer** (30 seconds EVE exposure time).

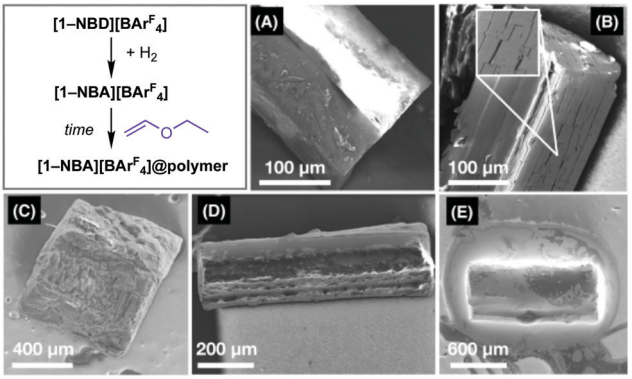

Fig. 2 SEM images of different single-crystal samples in polymer grafting-from experiments. (A) **[1-NBD][BArF4]**. (B) **[1-NBD][BArF4]** + H_2 to form **[1-NBA][BArF4]**. Inset shows microcracks. (C) **[1-NBA][BArF4]@poly-(ethylvinylether)** formed after exposure to EVE for 30 seconds, (D) 2.5 minutes EVE exposure. (E) 15 minutes EVE exposure.

Ethylvinylether (EVE) was chosen as the volatile monomer, due to its low boiling point (33 °C), well-established cationic polymerisation chemistry to form poly(ethylvinylether) using homogeneous[21,22] and heterogeneous catalysis,[23] and use in grafting-from processes on silica surfaces.[24] Two methodologies were developed to use discrete SMOM single-crystals under vapour-phase polymerisation conditions, Fig. 1.

For Method A, a single crystal of precursor **[1-NBD][BArF4]** (1.5 mg, 1 × 1 × 2 mm) was mounted, using a dab of silicon grease, on the side of a 50 cm^3 flask fitted with a PFTE greaseless stopcock and a glass insert to contain EVE monomer, Fig. 1B. The active catalyst, **[1-NBA][BArF4]**, was generated in a SC–SC transformation by adding H_2 (1 bar) for 30 min. H_2 was removed and EVE (0.15 cm^3, $[Rh]_{TOTAL}$: [monomer] ~ 1 : 1000) placed in the insert and the stopcock closed, generating a vapour atmosphere. After 15 minutes the formation of liquid polymer was observed around the crystal. Over a 48 h period this pooled at the bottom of the flask, removing it from the locus of the solid-catalyst. Analysis of this colourless oil by gel permeation chromatography (GPC) and NMR spectroscopy showed it to be atactic[21,25] poly(ethylvinylether): $M_{n(average)}$ = 21 500 g mol^{-1} ($Đ$ = 2.5).[26] While the crystal maintained visual integrity, after 15 minutes crystallinity was lost (*vide infra*). Using the same total mass of precursor but smaller crystals (3 × 0.5 mg, 0.5 × 0.5 × 1 mm) led to shorter polymer chains with a wider distribution ($M_{n(average)}$ = 10 900 g mol^{-1}, $Đ$ = 3.6), consistent with an increased number of surface initiating sites.[27] No polymerisation was observed using **[1-NBD][BArF4]**.

While this methodology allowed for bulk polymer to be prepared, a temporal analysis of the catalyst was challenging. This was overcome by a modification of the experimental procedure (Method B), in which 5–6 crystals of precursor **[1-NBD][BArF4]** (~1 mg each) were mounted on specially adapted PFTE stopcock fitted with a metal needle, Fig. 1C. This technique allowed for expedient analysis of crystalline SMOM@polymer by scanning electron microscopy (SEM), NMR spectroscopy and single-crystal X-ray diffraction; especially at the early stages of surface polymerisation (0–15 minutes). Longer reaction times resulted a viscous polymer drop forming that dissolved the catalyst (see ESI† for Movie).

SEM images of samples from these experiments are shown in Fig. 2. Precursor **[1-NBD][BArF4]** shows a clean, unpitted surface (Fig. 2A). While addition of H_2 to form **[1-NBA][BArF4]** is a SC–SC transformation,[16] significant microcracking of the surface of the crystal occurs (Fig. 2B) that likely opens up more initiating sites. This SEM analysis confirms previous suggestions made by ourselves,[17,20,28] and others,[29] for micro-cracking in solid/gas SMOM transformations. Analysis of the surface of **[1-NBA][BArF4]** by Energy-Dispersive X-ray spectroscopy (EDX) showed significant amounts of fluorine, consistent with the $-CF_3$ groups of the $[BAr^F_4]^-$ anion being at or near surface.

After 30 seconds exposure of **[1-NBA][BArF4]** to EVE vapour a polymer layer had formed on the surface of the crystal (Fig. 2C) giving **[1-NBA][BArF4]@poly(ethylvinylether)**. Fluorine is still observed by EDX, suggesting a polymer layer of <1–2 μm. Dissolving these crystals in MeCN solvent formed the previously reported complex $[Rh(Cy_2PCH_2CH_2PCy_2)(NCMe)_2][BAr^F_4]$:[17] $\delta^{31}P\{^1H\}$ = 91.0 [J(RhP) = 175 Hz]. In addition to this complex, in the ^{1}H NMR spectrum a low intensity, broad, resonance at δ 3.5 is observed that is assigned to the ether protons, $-CH(OCH_2CH_3)-$, of poly(ethylvinylether).[25] Integration relative to $[BAr^F_4]^-$ gives a ratio of 0.1 : 1 respectively. $^{31}P\{^1H\}$ solid-state NMR spectroscopy (SSNMR) of polymer-coated crystals shows that **[1-NBA][BArF4]** is the major species present, [δ 110.3, virtual triplet J(RhP) = 209, 214 Hz].[16] Additional signals at δ 105 and δ 80 are tentatively assigned to polymer-bound surface species.

After 2.5 minutes exposure to EVE vapour the polymer layer has increased, as shown by SEM (Fig. 2D), EDX that now reveals no fluorine, and in the ^{1}H NMR spectrum of the dissolved sample in which the polymer ether groups are now clearly observed: ratio with $[BAr^F_4]^-$ 0.7 : 1. Further exposure to EVE (15 minutes, Fig. 2E) results in a polymer corona around the sample, and an increase in the polymer ether signals in the ^{1}H NMR spectrum of dissolved material (ether : $[BAr^F_4]^-$ = 4.4 : 1).

Single crystallinity is retained in early stages of surface-polymerisation. After 30 seconds exposure to EVE (Fig. 2C) analysis

by single-crystal X-ray diffraction provides a very good refinement and solution for **[1-NBA][BAr$^F_4$]@poly(ethylvinylether)** (R = 7.5%) that is essentially isostructural with **[1-NBA][BAr$^F_4$]**.[16] After 2.5 minutes exposure (Fig. 2D) all high-angle data is lost and no structural refinement was possible. 15 minutes exposure to EVE resulted in complete loss of Bragg reflections.

The grafted-from polymer coating on **[1-NBA][BAr$^F_4$]@poly(ethylvinylether)** makes crystals of this σ-alkane complex remarkably tolerant to air. Fig. 3A and B compare single-crystalline samples of **[1-NBA][BAr$^F_4$]** with **[1-NBA][BAr$^F_4$]@poly(ethylvinylether)** formed after 30 seconds exposure to EVE, when both are contacted with air. For the uncoated samples there is a progressive colour change from red to green over 30 minutes, which is accompanied by a complete loss in diffraction and a $^{31}P\{^1H\}$ SSNMR spectrum that is broad and ill-defined. By contrast the polymer-coated crystals are air stable over this time as measured by $^{31}P\{^1H\}$ SSNMR and single-crystal X-ray diffraction. The resulting structural refinement for **[1-NBA][BAr$^F_4$]** is essentially no different from pristine sample synthesised under strict anaerobic conditions[16] (Fig. 3C, R = 4.9%). While longer contact times with air resulted in significant decomposition, low-angle Bragg peaks are still evident after 8 hours. Polymer matrices have been previously used to protect electrochemical hydrogen oxidation catalysts towards oxygen damage,[30] or stabilise MOF nanoparticles towards decomposition by air.[8]

The polymer coating in **[1-NBA][BAr$^F_4$]@poly(ethylvinylether)** allows for solid/gas SC–SC transformations to occur at the metal centre in the bulk crystal, albeit at an attenuated rate. Exposure to propene (1 bar, 298 K) for 5 days resulted in exchange of the NBA ligand for propene, to form **[1-propene][BAr$^F_4$]@poly(ethylvinylether)**, in a SC–SC transformation. This is much slower than for uncoated crystals (2 h[17]) consistent with the polymer layer, as measured by NMR spectroscopy. The structural refinement (R = 10%) shows a propene ligand bound through alkene and agostic Rh···H_3C groups, as reported for unfunctionalised **[1-propene][BAr$^F_4$]**.[17]

A possible mechanism for the surface-initiated cationic polymerisation of EVE is shown in Fig. 4. $[Rh(Cy_2PCH_2CH_2PCy_2)(NBA)]^+$ cations close to the surface undergo rapid substitution with EVE to form an intermediate such as **A**, similar to those proposed as initiating sites for homogeneous cationic polymerisations using transition metal complexes.[22] Chain-propagation then leads to polymer brushes[1] and the resulting SMOM@polymer. Mechanical stress from growing polymer chains may well lead to detachment from the crystal surface over time, which would also contribute to the observed loss in crystallinity.

In support of this mechanism we have characterised a model complex for intermediate **A** by using diethyl ether as a saturated analogue of EVE, that mimics initiation but does not propagate. Fig. 5 shows the synthetic methodology and solid-state structure of $[Rh(Cy_2PCH_2CH_2PCy_2)(Et_2O)][BAr^F_4]$, **[1-Et$_2$O][BAr$^F_4$]** formed by exposing crystalline **[1-NBA][BAr$^F_4$]** to diethyl ether vapour for 24 hours after which excess vapour is removed with an argon flush.[31] Unsurprisingly, **[1-NBD][BAr$^F_4$]** was unreactive. The cation is a pseudo square planar $\{Rh(L_2)\}^+$ fragment bound with a diethyl ether ligand, through Rh–O [2.204(6) Å] and γ-agostic[32] Rh···H_3C [Rh–C27, 2.522(9) Å] interactions. Reflecting the different *trans* influence of ether *versus* agostic groups, Rh–P1 is shorter than Rh–P2. In the $^{31}P\{^1H\}$ SSNMR spectrum two sharp environments are observed at δ 107.0 [J(RhP) = 201 Hz] and 99.2 [J(RhP) = 223 Hz], the latter assigned to P1 on the basis of the larger coupling to ^{103}Rh. While the formation of **[1-Et$_2$O][BAr$^F_4$]** from **[1-NBA][BAr$^F_4$]** is a SC–SC process, the amorphous $[BAr^F_4]$-coordinated zwitterion $[Rh(Cy_2PCH_2CH_2PCy_2)\{(\eta^6\text{-}(F_3C)_2C_6H_3)BAr^F_3\}]$ **[1-BAr$^F_4$]**[16] is also formed by subsequent loss of Et_2O,[31] as signalled in the $^{31}P\{^1H\}$ SSNMR spectrum by a broad peak at δ 91. This hampers further solid-state reactivity studies of **[1-Et$_2$O][BAr$^F_4$]**. It is also not stable solution and dissolving in cold CD_2Cl_2 or Et_2O (183 K)

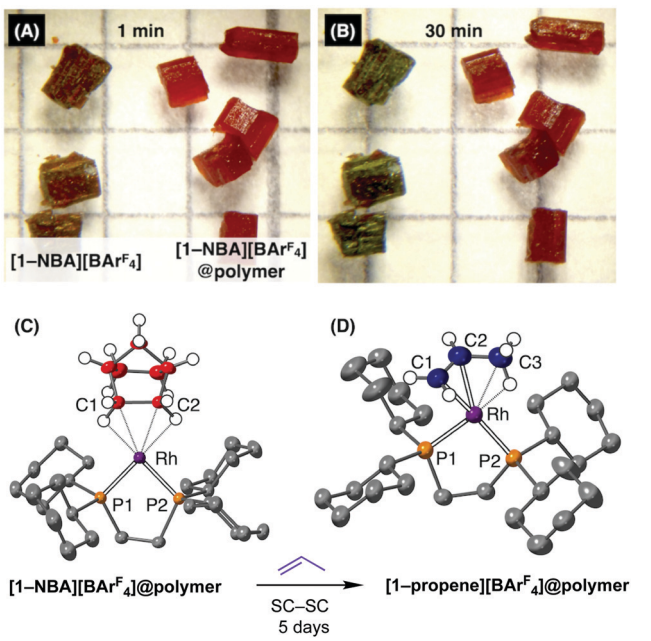

Fig. 3 Optical images of samples of **[1-NBA][BAr$^F_4$]** (left) and **[1-NBA][BAr$^F_4$]@poly(ethylvinylether)** (right, 30 seconds EVE vapour) after: (A) 1 minute exposure to air and (B) 30 minutes exposure to air. Grid = 2 × 2 mm. (C) Solid-state molecular structure of the cation in **[1-NBA][BAr$^F_4$]@poly(ethylvinylether)** (30 minutes exposure to air). (D) Solid-state molecular structure of the cation in **[1-propene][BAr$^F_4$]@poly(ethylvinylether)** (only one disordered component shown).

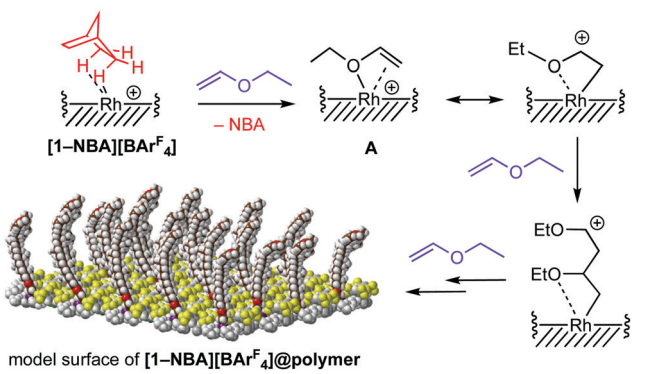

Fig. 4 Suggested mechanism of grafting-from cationic surface polymerisation to form **[1-NBA][BAr$^F_4$]@poly(ethylvinylether)**. $[BAr^F_4]^-$ anions not drawn.

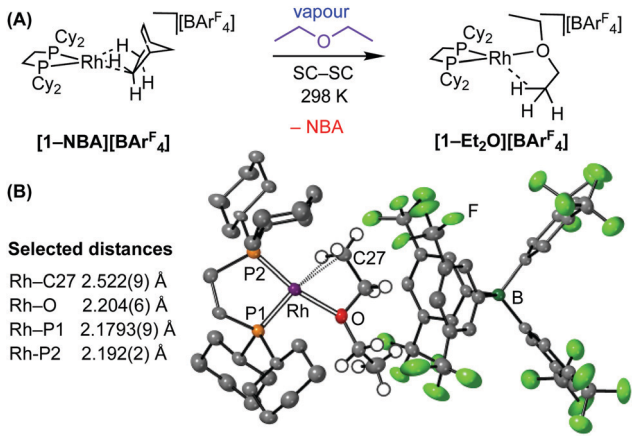

Fig. 5 (A) Synthesis of **[1-Et$_2$O][BAr$^F_4$]** from **[1-NBA][BAr$^F_4$]**. (B) Solid-state molecular structure of **[1-Et$_2$O][BAr$^F_4$]** with selected bond distances. Hydrogen atoms in calculated positions. See ESI.†

results in the formation **[1-BAr$^F_4$]**. While structurally characterised diethyl ether complexes are known,[33] **[1-Et$_2$O][BAr$^F_4$]** is the first example of a diethyl ether complex that also contains an agostic interaction.

In summary, vapour phase grafting-from SMOM@polymer method provides a simple method for stabilisation of reactive, crystalline, molecular organometallic species towards air while also allowing for single-crystal structural determinations and retaining bulk SC–SC reactivity. That this methodology results in a σ-alkane complex becoming air tolerant in the solid-state further extends the potential use of these fascinating, and reactive,[15] complexes as precursors in synthesis and catalysis.[28]

We thank the EPSRC (EP/M024210), Leverhulme Trust (RPG-2015-447) and SCG Chemicals for funding.

Conflicts of interest

There are no conflicts to declare.

Notes and references

1 W.-L. Chen, R. Cordero, H. Tran and C. K. Ober, *Macromolecules*, 2017, **50**, 4089–4113.
2 L. Michalek, L. Barner and C. Barner-Kowollik, *Adv. Mater.*, 2018, **30**, 1706321; J. Cai, C. Li, N. Kong, Y. Lu, G. Lin, X. Wang, Y. Yao, I. Manners and H. Qiu, *Science*, 2019, **366**, 1095–1098.
3 C. M. Hui, J. Pietrasik, M. Schmitt, C. Mahoney, J. Choi, M. R. Bockstaller and K. Matyjaszewski, *Chem. Mater.*, 2014, **26**, 745–762; *Surface-Initiated Polymerization I*, ed. R. Jordan, Springer, Berlin, 2006.
4 N. Rubio, H. Au, H. S. Leese, S. Hu, A. J. Clancy and M. S. P. Shaffer, *Macromolecules*, 2017, **50**, 7070–7079.
5 M. Steenackers, I. D. Sharp, K. Larsson, N. A. Hutter, M. Stutzmann and R. Jordan, *Chem. Mater.*, 2010, **22**, 272–278.
6 G. Bissadi and R. Weberskirch, *Polym. Chem.*, 2016, **7**, 5157–5168.
7 S. He, H. Wang, C. Zhang, S. Zhang, Y. Yu, Y. Lee and T. Li, *Chem. Sci.*, 2019, **10**, 1816–1822.
8 L. Hou, L. Wang, N. Zhang, Z. Xie and D. Dong, *Polym. Chem.*, 2016, **7**, 5828–5834.
9 Q. T. Easter, V. Trauschke and S. A. Blum, *ACS Catal.*, 2015, **5**, 2290–2295.
10 M. Asai, D. Zhao and S. K. Kumar, *ACS Nano*, 2017, **11**, 7028–7035.
11 Y. Takashima, H. N. Miras, S. Glatzel and L. Cronin, *Chem. Commun.*, 2016, **52**, 7794–7797.
12 S. S. Jeon, J. K. Park, C. S. Yoon and S. S. Im, *Langmuir*, 2009, **25**, 11420–11424.
13 R. Muramatsu, Y. Oaki, K. Kuwabara, K. Hayashi and H. Imai, *Chem. Commun.*, 2014, **50**, 11840–11843.
14 A. Fast, N. M. Esfandiari and S. A. Blum, *ACS Catal.*, 2013, **3**, 2150–2153.
15 A. J. Cowan and M. W. George, *Coord. Chem. Rev.*, 2008, **252**, 2504–2511; A. S. Weller, F. M. Chadwick and A. I. McKay, in *Advances in Organometallic Chemistry*, ed. P. J. Pérez, Academic Press, 2016, vol. 66, pp. 223–276.
16 S. D. Pike, F. M. Chadwick, N. H. Rees, M. P. Scott, A. S. Weller, T. Krämer and S. A. Macgregor, *J. Am. Chem. Soc.*, 2015, **137**, 820–833.
17 F. M. Chadwick, A. I. McKay, A. J. Martínez-Martínez, N. H. Rees, T. Krämer, S. A. Macgregor and A. S. Weller, *Chem. Sci.*, 2017, **8**, 6014–6029.
18 A. I. McKay, A. J. Bukvic, B. E. Tegner, A. L. Burnage, A. J. Martínez-Martínez, N. H. Rees, S. A. Macgregor and A. S. Weller, *J. Am. Chem. Soc.*, 2019, **141**, 11700–11712.
19 A. J. Martínez-Martínez, N. H. Rees and A. S. Weller, *Angew. Chem., Int. Ed.*, 2019, **58**, 16873–16877.
20 S. D. Pike, T. Krämer, N. H. Rees, S. A. Macgregor and A. S. Weller, *Organometallics*, 2015, **34**, 1487–1497.
21 P. J. Albietz, K. Yang and R. Eisenberg, *Organometallics*, 1999, **18**, 2747–2749.
22 C. Chen, S. Luo and R. F. Jordan, *J. Am. Chem. Soc.*, 2010, **132**, 5273–5284.
23 A. Kanazawa, S. Kanaoka and S. Aoshima, *J. Polym. Sci., Part A: Polym. Chem.*, 2010, **48**, 916–926.
24 S. Spange, U. Eismann, S. Höhne and E. Langhammer, *Macromol. Symp.*, 1997, **126**, 223–236; U. Eismann and S. Spange, *Macromolecules*, 1997, **30**, 3439–3446.
25 K. Matsuzaki, H. Ito, T. Kawamura and T. Uryu, *J. Polym. Sci.*, 1973, **11**, 971–987.
26 Distinct polymer end groups such as aldehyde and acetal were not observed. The mechanism termination/chain transfer is undetermined.
27 We cannot discount a small amount of soluble catalyst is formed, that would be increased when using crystals of a higher surface area.
28 A. J. Martínez-Martínez, C. G. Royle, S. K. Furfari, K. Suriye and A. S. Weller, *ACS Catal.*, 2020, **10**, 1984–1992.
29 M. Oliván, A. V. Marchenko, J. N. Coalter and K. G. Caulton, *J. Am. Chem. Soc.*, 1997, **119**, 8389–8390.
30 A. A. Oughli, A. Ruff, N. P. Boralugodage, P. Rodríguez-Maciá, N. Plumeré, W. Lubitz, W. J. Shaw, W. Schuhmann and O. Rüdiger, *Nat. Commun.*, 2018, **9**, 864.
31 Shorter reaction times resulted in **[1-NBA][BAr$^F_4$]** still being present, while exposure to vacumm overnight results in significantly more **[1-BAr$^F_4$]** being formed.
32 M. Brookhart, M. L. H. Green and G. Parkin, *Proc. Natl. Acad. Sci. U. S. A.*, 2007, **104**, 6908–6914; H. Urtel, C. Meier, F. Eisenträger, F. Rominger, J. P. Joschek and P. Hofmann, *Angew. Chem., Int. Ed.*, 2001, **40**, 781–784.
33 J. Ledford, C. S. Shultz, D. P. Gates, P. S. White, J. M. DeSimone and M. Brookhart, *Organometallics*, 2001, **20**, 5266–5276.